Contribution from the Department of Chemistry,
Harvard University, Cambridge, Massachusetts 02138

Alternative Spin States in Synthetic Analogues of Biological Clusters: Spin-Quartet Ground States and Structures of $[Fe_4S_4(SPh)_4]^{3-}$ and $[Fe_4Se_4(SPh)_4]^{3-}$ as Their Tetramethylammonium Salts

M. J. Carney,[1a] G. C. Papaefthymiou,[1b] M. A. Whitener,[1a] K. Spartalian,[1b,c] R. B. Frankel,[1b] and R. H. Holm*[1a]

Received September 11, 1987

The compounds $(Me_4N)_3[Fe_4X_4(SPh)_4]\cdot 2MeCN$ [X = S (**1**), Se (**2**)] were prepared in good yields by chemical reduction of the corresponding dianion cluster salts and were thoroughly characterized as part of an investigation of alternative spin states in cubane-type clusters having the $[Fe_4(\mu_3\text{-}X)_4]^+$ core. Clusters with this core unit are found in reduced ferredoxins and other Fe-S proteins and enzymes. The two compounds obey the Curie-Weiss law over the temperature ranges 2.1-15 K (**1**) and 7.0-50 K (**2**) with Curie constants of 1.891 (**1**) and 1.883 (**2**) emu K/G, consistent with a $S = {}^3/_2$ ground state. Magnetization behaviors between 1.8 and 100 K and at fields up to 50 kOe were successfully analyzed in terms of a spin Hamiltonian with $S = {}^3/_2$. Mössbauer spectra revealed isomer shifts similar to those of other reduced clusters and independent of chalcogenide atom X, very small magnetic splittings in large applied magnetic fields, and negative hyperfine fields at all ^{57}Fe sites. Compound **1** crystallizes in monoclinic space group $C2/c$ with $a = 22.868$ (6) Å, $b = 11.211$ (2) Å, $c = 20.387$ (4) Å, $\beta = 90.08$ (2)°, and $Z = 4$. Compound **2** was obtained in orthorhombic space group $Fdd2$ with $a = 39.386$ (8) Å, $b = 23.991$ (5) Å, $c = 11.471$ (2) Å, and $Z = 8$. Refinement of compounds **1**/**2** with use of 2839/1957 unique data converged at $R = 4.44\%/3.32\%$. Clusters **1** and **2** have very similar structures. Core Fe-X bond lengths may be organized into a set of four long plus eight short with mean values (Å) of 2.344 (6) + 2.287 (19) for **1** and 2.488 (4) + 2.403 (12) for **2**, with the long bonds approximately perpendicular to the direction of a C_2 axis crystallographically imposed in each case. The cores have tetragonally elongated (D_{2d}) configurations with the elongation along the direction of an idealized $\bar{4}$ axis. The magnetic and spectroscopic results, together with crystallographic definition of the clusters, establish beyond question that the reduced clusters $[Fe_4X_4(SPh)_4]^{3-}$ (X = S, Se) can stabilize electronic configurations with spin-quartet ground states. Examples of "nonstandard" biological clusters with $S > {}^1/_2$ are cited, including the $S = {}^3/_2$ cluster of the Fe protein of *Azotobacter vinelandii* nitrogenase. All aspects of the present work support the published spin-state assignment of this cluster. While it may be significant that **1** and **2** have elongated tetragonal cores and $S = {}^3/_2$ ground states, examination of all results for reduced clusters does not yet afford a clear spin-state-structure correlation.

Introduction

A portion of our prior research on biologically relevant iron-sulfur clusters[2] has resulted in the synthesis and characterization of a variety of clusters $[Fe_4S_4(SR)_4]^{3-}$[3-12] whose $[Fe_4S_4]^+$ cores are isoelectronic with reduced 4Fe-4S centers in many proteins and enzymes.[13,14] Consequently, these clusters serve as synthetic analogues of the reduced $Fe_4S_4(Cys\text{-}S)$ sites in biomolecules. This relationship is of particular significance because the $[Fe_4S_4]^{2+,+}$ core oxidation-level change is that of a widespread biological redox reaction wherein the clusters act as electron-transfer centers. It remains a significant matter to determine cluster structural and electronic changes pursuant to electron transfer, in order to acquire a detailed description of this pervasive redox process. Examination of analogues in solution provides a means of determining these changes in the absence of any perturbing effects of protein structure. In their crystalline states, however, perturbations influencing intrinsic properties are not necessarily absent. In this event, the forces associated with crystalline environments may lead to small but definite structural changes and corresponding variations in electronic features.

It has become evident that both natural and synthetic reduced clusters possess a variability of structural and electronic properties not yet detected in oxidized clusters containing the $[Fe_4S_4]^{2+}$ core. "Nonstandard" biological clusters[12] deviate from the usual spin-doublet ground state and associated Mössbauer spectroscopic properties. Among these are the $[Fe_4Se_4]^+$ clusters of the selenium-reconstituted reduced ferredoxin ($Se\text{-}Fd_{red}$) from *Clostridium pasteurianum*, which has been prepared and studied in considerable detail by Meyer and co-workers.[15-22] Synthetic clusters $[Fe_4S_4(SR)_4]^{3-}$ do not exhibit uniform structures and electronic properties in the solid state. Recently, we have been able to show that such clusters as crystalline salts may exist in $S = {}^1/_2$ or ${}^3/_2$ ground states, as deduced from low-temperature magnetization and magnetic susceptibility properties.[12] This finding and the data upon which it is based fully support the conclusion that the Fe protein of nitrogenase contains an $[Fe_4S_4]^+$ cluster with $S = {}^3/_2$.[23] Further, spectroscopic evidence indicates that certain $[Fe_4Se_4]^+$ clusters in $Se\text{-}Fd_{red}$ populate states with $S \geq {}^3/_2$.[19-22]

In this investigation we provide additional evidence for $[Fe_4S_4]^+$ clusters, and the first unambiguous evidence for $[Fe_4Se_4]^+$ clusters, of ground states with spin $S > {}^1/_2$. These conclusions are drawn from a combination of magnetization, magnetic susceptibility, and Mössbauer spectroscopic results for crystalline Me_4N^+ salts of

(1) (a) Harvard University. (b) Francis Bitter National Magnet Laboratory, Massachusetts Institute of Technology. (c) University of Vermont.
(2) Berg, J. M.; Holm, R. H. In *Metals Ions in Biology*; Spiro, T. G., Ed.; Interscience: New York, 1982; Vol. 4, Chapter 1.
(3) Cambray, J.; Lane, R. W.; Wedd, A. G.; Johnson, R. W.; Holm, R. H. *Inorg. Chem.* **1977**, *16*, 2565.
(4) Reynolds, J. G.; Laskowski, E. J.; Holm, R. H. *J. Am. Chem. Soc.* **1978**, *100*, 5315.
(5) Laskowski, E. J.; Frankel, R. B.; Gillum, W. O.; Papaefthymiou, G. C.; Renaud, J.; Ibers, J. A.; Holm, R. H. *J. Am. Chem. Soc.* **1978**, *100*, 5322.
(6) Berg, J. M.; Hodgson, K. O.; Holm, R. H. *J. Am. Chem. Soc.* **1979**, *101*, 4586.
(7) Laskowski, E. J.; Reynolds, J. G.; Frankel, R. B.; Foner, S.; Papaefthymiou, G. C.; Holm, R. H. *J. Am. Chem. Soc.* **1979**, *101*, 6562.
(8) Reynolds, J. G.; Coyle, C. L.; Holm, R. H. *J. Am. Chem. Soc.* **1980**, *102*, 4350.
(9) Papaefthymiou, G. C.; Laskowski, E. J.; Frota-Pessôa, S.; Frankel, R. B.; Holm, R. H. *Inorg. Chem.* **1982**, *21*, 1723.
(10) Stephan, D. W.; Papaefthymiou, G. C.; Frankel, R. B.; Holm, R. H. *Inorg. Chem.* **1983**, *22*, 1550.
(11) Hagen, K. S.; Watson, A. D.; Holm, R. H. *Inorg. Chem.* **1984**, *23*, 2984.
(12) Carney, M. J.; Holm, R. H.; Papaefthymiou, G. C.; Frankel, R. B. *J. Am. Chem. Soc.* **1986**, *108*, 3519.
(13) Sweeney, W. V.; Rabinowitz, J. C. *Annu. Rev. Biochem.* **1980**, *49*, 39.
(14) Thomson, A. J. *Top. Mol. Struct. Biol.* **1985**, *6*, 79.
(15) Meyer, J.; Moulis, J.-M. *Biochem. Biophys. Res. Commun.* **1981**, *103*, 667.
(16) Moulis, J.-M.; Meyer, J. *Biochemistry* **1982**, *21*, 4762.
(17) Moulis, J.-M.; Meyer, J.; Lutz, M. *Biochem. J.* **1984**, *219*, 829.
(18) Moulis, J.-M.; Meyer, J. *Biochemistry* **1984**, *23*, 6605.
(19) Moulis, J.-M.; Auric, P.; Gaillard, J.; Meyer, J. *J. Biol. Chem.* **1984**, *259*, 11396.
(20) Gaillard, J.; Moulis, J.-M.; Auric, P.; Meyer, J. *Biochemistry* **1986**, *25*, 464.
(21) Gaillard, J.; Moulis J.-M.; Meyer, J. *Inorg. Chem.* **1987**, *26*, 320.
(22) Auric, P.; Gaillard, J.; Meyer, J.; Moulis, J.-M. *Biochem. J.* **1987**, *242*, 525.
(23) Lindahl, P. A.; Day, E. P.; Kent, T. A.; Orme-Johnson, W. H.; Münck, E. *J. Biol. Chem.* **1985**, *260*, 11160.

0020-1669/88/1327-0346$01.50/0

$[Fe_4S_4(SPh)_4]^{3-}$ and $[Fe_4Se_4(SPh)_4]^{3-}$, whose crystal structures are also reported here.

Experimental Section

Preparation of Compounds. All manipulations were carried out under a pure dinitrogen atmosphere. Solvents were degassed prior to use. $(Me_4N)_2[Fe_4S_4(SPh)_4]$[24] and $(Me_4N)_2[Fe_4Se_4(SPh)_4]$[25] were prepared as previously described. Reduced cluster compounds were obtained by reduction of these salts with sodium acenaphthylenide as described earlier[3] but with acetonitrile rather than hexamethylphosphoramide as the solvent.

(a) $(Me_4N)_3[Fe_4S_4(SPh)_4]\cdot 2MeCN$. To a solution of 2.00 g (2.10 mmol) of $(Me_4N)_2[Fe_4S_4(SPh)_4]$ in 75 mL of acetonitrile was added a small excess (1.2 equiv) of sodium acenaphthylenide in THF dropwise with stirring. After the addition of 0.23 g (2.1 mmol) of Me_4NCl, the mixture was stirred overnight, warmed to 50 °C, and filtered to remove NaCl. Slow cooling of the filtrate to −20 °C produced large black crystalline blocks. These were collected by filtration, washed with THF, and dried in vacuo, affording 1.20 g (54%) of pure product. Anal. Calcd for $C_{40}H_{62}Fe_4N_5S_8$: C, 43.96; H, 5.72; Fe, 20.44; N, 6.41; S, 23.47. Found: C, 44.00; H, 5.64; Fe, 20.51; N, 6.28; S, 23.36. ^1H NMR (Me_2SO-d_6, 298 K): 10.4 (*m*-H), 3.11 (NMe), 2.17 (*o*-H), 1.63 ppm (*p*-H).

(b) $(Me_4N)_3[Fe_4Se_4(SPh)_4]\cdot 2MeCN$. This compound was prepared analogously to the preceding compound and was obtained as large black needles in 68% yield. Anal. Calcd for $C_{40}H_{62}Fe_4N_5S_4Se_4$: C, 37.52; H, 4.88; Fe, 17.45; N, 5.47; S, 10.02; Se, 24.67. Found: C, 37.44; H, 4.90; Fe, 17.50; N, 5.36; S, 10.14; Se, 24.53. ^1H NMR (Me_2SO, 298 K): 11.6 (*m*-H), 3.11 (NMe), −0.61 ppm (*o*-, *p*-H).

These compounds are extremely air-sensitive, especially in solution. Chemical shifts compare closely with previous values,[4,8] indicating full reduction of the dianion clusters. The Me_4N^+ salt of $[Fe_4Se_4(S\text{-}p\text{-}C_6H_4Me)_4]^{3-}$[8] is the only previously isolated $[Fe_4Se_4]^+$ cluster.

Physical Measurements. All measurements were performed under strictly anaerobic conditions. Magnetic susceptibility and magnetization measurements at applied fields of 5 kOe and up to 50 kOe, respectively, were carried out on an SHE 905 SQUID magnetometer operating between 1.8 and 300 K. Finely ground samples of ca. 20–30 mg were loaded into precalibrated containers, dispersed with 30 μL of toluene, and sealed under a He atmosphere with epoxy resin. Dispersal in toluene was found to be necessary, as crystallites in polycrystalline samples tended to orient in large applied fields at low temperature, producing anomalously high magnetic moments. This alignment was permanent and varied from sample to sample. Dispersed samples gave moments reproducible to ±1% at all values of the applied field.[26] Moments at 5 kOe and 6 K determined before and after cycling through higher fields and lower temperatures were identical. Diamagnetic susceptibility corrections[27] were applied. Mössbauer spectra were determined with a constant-acceleration spectrometer equipped with a ^{57}Co source in a Rh matrix. Magnetically perturbed spectra were obtained in longitudinally applied fields up to 80 kOe with the source and absorber at 4.2 K. Zero-field measurements were made at 4.2 and 80 K with the spectrometer operating in the time mode and the source maintained at room temperature. Polycrystalline samples were dispersed in boron nitride powder and sealed in plastic sample holders. Samples were also dispersed in toluene and Nujol mulls. Spectra were the same for each type of sample preparation and showed no preferential crystallite orientation. EPR spectra were recorded at X-band frequencies and ~9 K on a Varian E-109 spectrometer equipped with a Helitran Model LTD-3-110 temperature controller.

Collection and Reduction of X-ray Data. Single crystals of $(Me_4N)_3[Fe_4S_4(SPh)_4]\cdot 2MeCN$ (**1**) were obtained by diffusing THF into a dilute acetonitrile solution of the compound. Single crystals of $(Me_4N)_3[Fe_4Se_4(SPh)_4]\cdot 2MeCN$ (**2**) were grown by slow cooling of the filtrate from the reaction mixture. The crystals were sealed in glass capillaries under a dinitrogen atmosphere. Data collections were carried out at ambient temperature on a Nicolet P3F automated four-circle diffractometer equipped with a graphite monochromator. Data collection parameters are provided in Table I. Orientation matrices and unit cell parameters were obtained from 25 machine-centered reflections ($20° \le 2\theta \le 25°$). Intensities of three check reflections were monitored every 123 reflections; no significant decay was observed over the course of data collection. Data sets were processed with the program XTAPE of the SHELXTL program package (Nicolet XRD Corp., Madison, WI), and empirical absorption corrections were applied to **1** and **2** by using the programs PSICOR and XEMP, respectively. For compound **1**, axial photographs and the systematic absences hkl ($h + k = 2n + 1$), $h0l$ ($h, l = 2n + 1$), and $0k0$ ($k = 2n + 1$) are consistent with the monoclinic space groups *Cc* (No. 9) and *C*2/*c* (No. 15); simple *E* statistics favored the centrosymmetric space group *C*2/*c*. Successful solution and refinement of the structure proved this choice to be correct. For compound **2**, the observed systematic absences are consistent only with orthorhombic space group *F*2*dd*. The data were transformed to the standard setting *Fdd*2 (No. 43).

Table I. Summary of Crystal Data, Intensity Collection, and Structure Refinement Parameters for $(Me_4N)_3[Fe_4S_4(SC_6H_5)_4]\cdot 2MeCN$ (**1**) and $(Me_4N)_3[Fe_4Se_4(SC_6H_5)_4]\cdot 2MeCN$ (**2**)

	1	**2**
formula	$C_{40}H_{62}Fe_4S_8N_5$	$C_{40}H_{62}Fe_4Se_4S_4N_5$
mol wt	1092.87	1280.46
a, Å	22.868 (6)	39.386 (8)
b, Å	11.211 (2)	23.991 (5)
c, Å	20.387 (4)	11.471 (2)
β, deg	90.08 (2)	
cryst system	monoclinic	orthorhombic
V, Å^3	5226 (2)	10839 (4)
Z	4	8
d_{calcd}, g/cm^3	1.39	1.57
d_{obsd}, g/cm^3	1.39[a]	1.56[a]
space group	*C*2/*c*	*Fdd*2
cryst dimens, mm	0.45 × 0.40 × 0.25	0.50 × 0.40 × 0.30
radiation	Mo Kα (λ = 0.71069 Å)	Mo Kα (λ = 0.71069 Å)
abs coeff μ, cm^{-1}	14.3	38.9
scan speed, deg/min	2.0–29.3 (ω scan)	2.0–29.3 (ω scan)
scan range, deg	0.6 below $K\alpha_1$ to 0.6 above $K\alpha_2$	0.6 below $K\alpha_1$ to 0.6 above $K\alpha_2$
bkgd/scan time ratio	0.25	0.25
2θ limits	$3° \le 2\theta \le 50°$	$3° \le 2\theta \le 50°$
no. of data collcd	5125 ($+h,+k,\pm l$)	10991 ($+h,+k,+l$)
R_{merge},[b] %	1.95	1.37
no. of unique data ($F_o^2 > 3.0\sigma(F_o^2)$)	2839	1957
no. of variables	259	258
R (R_w),[c] %	4.44 (4.83)[d]	3.32 (3.80)[d]

[a] Determined by the neutral buoyancy method in CCl_4/hexane. [b] $R_{merge} = [\sum(N_i\sum_{j=1}^{N_i}(F_i - F_j))/\sum(N_i\sum_{j=1}^{N_i}F_j)]$, where N_i is the number of equivalent reflections merged to give the mean, $\bar{F}_i$, F_j is any one member of this set, and the calculations are done on a scale of F_o^2. [c] $R = \sum||F_o| - |F_c||/\sum|F_o|$; $R_w = [\sum w(|F_o|^2 - |F_c|^2)/\sum w|F_o|^2]^{1/2}$. [d] Weighting scheme for least-squares refinement: $w = (F_o/P(1))^2$, $F_o \le P(1)$; $w = (P(1)/F_o)^2$, $F_o > P(1)$; $P(1) = F(\min(|F_o|^2 - |F_c|^2)) = 22.0$ (20.0) for **1** (**2**).

Structure Solution and Refinement. Atomic scattering factors were taken from tabulated data.[28] The Fe and bridging S atoms of **1** and the Fe and bridging Se atoms of **2** were located by the direct-methods program MULTAN.[29] All remaining non-hydrogen atoms were found by Fourier maps and refined by using CRYSTALS.[30] For each compound, the asymmetric unit consists of one-half anion, one and one-half cations, and one acetonitrile solvate molecule. No disorder was evident, although the solvate molecules did require large thermal ellipsoids in both structures. Phenyl rings were treated as semirigid bodies and cations were constrained by the method of additional observational equations,[31] throughout both refinements. For **2**, the origin was fixed by setting the *z* coordinate of Se(1) equal to zero. Isotropic refinements converged at the conventional *R* values of 9.1% (**1**) and 8.6% (**2**). All non-hydrogen atoms were described anisotropically; hydrogen atoms were included at 0.95 Å from, and with isotropic thermal parameters 1.2 times those of, bonded carbon atoms. No hydrogen atoms were included on the solvate molecules. For **2**, inversion of the coordinates through ($^1/_8$, $^1/_8$, $^1/_8$) and

(24) Que, L., Jr.; Bobrik, M. A.; Ibers, J. A.; Holm, R. H. *J. Am. Chem. Soc.* **1974**, *96*, 4168.
(25) Bobrik, M. A.; Laskowski, E. J.; Johnson, R. W.; Gillum, W. O.; Berg, J. M.; Hodgson, K. O.; Holm, R. H. *Inorg. Chem.* **1978**, *17*, 1402.
(26) See paragraph at end of this article regarding supplementary material.
(27) O'Connor, C. J. *Prog. Inorg. Chem.* **1982**, *29*, 203.
(28) Cromer, D. T.; Waber, J. T. *International Tables for X-ray Crystallography*; Kynoch: Birmingham, England, 1974.
(29) Main, P.; Fiske, S. J.; Hull, S. E.; Lessinger, L.; Germain, G.; Declerq, J.-P.; Woolfson, M. M. "MULTAN-80, A System of Computer Programs for the Automatic Solution of Crystal Structures from X-ray Diffraction Data"; Universities of York and Louvain, 1980.
(30) Watkin, D. J.; Carruthers, J. R. "CRYSTALS Users Manual"; Chemical Crystallography Laboratory, Oxford University, 1984.
(31) Waser, J. *Acta Crystallogr.* **1963**, *16*, 1091.

Table II. Positional Parameters (×10⁴) for $(Me_4N)_3[Fe_4S_4(SC_6H_5)_4]\cdot 2MeCN$

atom	x/a	y/b	z/c
Fe(1)	577.2 (3)	604.7 (7)	2338.2 (4)
Fe(2)	159.6 (3)	2346.0 (7)	3139.4 (3)
S(1)	1233.7 (8)	−825 (2)	2015.9 (9)
S(2)	230.9 (8)	3759 (2)	3957.5 (8)
S(3)	789.3 (6)	2581.(1)	2271.5 (7)
S(4)	214.4 (6)	376 (1)	3385.7 (7)
N(3)	5000	1447 (6)	2500
N(4)	1082 (2)	1550 (6)	−22 (2)
N(5)	2738 (6)	643 (12)	560 (7)
C(11)	1811 (2)	−782 (4)	2593 (3)
C(12)	2137 (2)	−1811 (5)	2695 (3)
C(13)	2617 (3)	−1797 (6)	3110 (3)
C(14)	2780 (3)	−761 (6)	3431 (3)
C(15)	2449 (2)	257 (6)	3337 (3)
C(16)	1967 (2)	254 (5)	2921 (3)
C(21)	792 (2)	3329 (5)	4502 (2)
C(22)	795 (3)	3822 (6)	5128 (2)
C(23)	1224 (3)	3483 (7)	5572 (3)
C(24)	1656 (3)	2676 (7)	5397 (3)
C(25)	1666 (3)	2199 (6)	4772 (3)
C(26)	1230 (2)	2522 (5)	4333 (3)
C(31)	4484 (4)	704 (7)	2650 (4)
C(32)	5127 (4)	2211 (7)	3072 (4)
C(41)	1339 (4)	2305 (13)	486 (5)
C(42)	547 (6)	2056 (14)	−249 (5)
C(43)	911 (6)	349 (13)	257 (6)
C(44)	1499 (4)	1295 (10)	−569 (4)
C(51)	2909 (5)	214 (10)	1035 (8)
C(52)	3122 (6)	−294 (13)	1622 (5)

Table III. Positional Parameters (×10⁴) for $(Me_4N)_3[Fe_4Se_4(SC_6H_5)_4]\cdot 2MeCN$

atom	x/a	y/b	z/c
Se(1)	−20.2 (2)	839.5 (3)	0
Se(2)	501.3 (2)	73.3 (3)	2289.0 (9)
Fe(1)	344.2 (3)	41.0 (5)	283 (1)
Fe(2)	−19.4 (3)	583.2 (4)	2027 (1)
S(1)	737.1 (6)	−149 (1)	−1129 (2)
S(2)	−156.9 (7)	1212 (1)	3487 (2)
N(3)	0	0	6191 (9)
N(4)	1208 (2)	1331 (3)	3842 (8)
N(5)	967 (5)	2263 (6)	6966 (18)
C(11)	1047 (2)	380 (3)	−1266 (6)
C(12)	1261 (2)	372 (4)	−2230 (7)
C(13)	1514 (2)	769 (4)	−2353 (10)
C(14)	1550 (2)	1176 (4)	−1505 (11)
C(15)	1338 (2)	1191 (4)	−539 (10)
C(16)	1086 (2)	790 (3)	−422 (7)
C(21)	92 (2)	1826 (3)	3409 (6)
C(22)	216 (2)	2032 (3)	2358 (7)
C(23)	386 (2)	2540 (3)	2325 (9)
C(24)	431 (2)	2853 (4)	3332 (9)
C(25)	309 (2)	2647 (3)	4383 (9)
C(26)	141 (2)	2138 (3)	4418 (7)
C(31)	−17 (3)	517 (5)	6921 (11)
C(32)	307 (3)	20 (5)	5443 (10)
C(41)	1138 (3)	1945 (6)	3893 (15)
C(42)	1546 (4)	1249 (6)	4262 (22)
C(43)	960 (4)	1000 (7)	4524 (13)
C(44)	1195 (6)	1136 (8)	2599 (17)
C(51)	756 (5)	2058 (7)	7570 (18)
C(52)	518 (4)	1881 (9)	8347 (22)

re-refinement of the thermal parameters to convergence yielded an R value of 3.47%, indicating that the initial choice of polarity (R = 3.32%) was correct. Final difference Fourier maps showed no peaks larger than 0.44 e/Å³ (**1**) and 0.42 e/Å³ (**2**). Final R values are given in Table I, and atom positional parameters are listed in Tables II and III.[26]

Results and Discussion

In our continuing study of the electronic properties of reduced clusters, we have sought examples of $[Fe_4S_4(SR)_4]^{3-}$ and $[Fe_4Se_4(SR)_4]^{3-}$ species with ground states of spin greater than $^1/_2$, preferably in constitutively analogous compounds. This requirement has been admirably met by the compounds

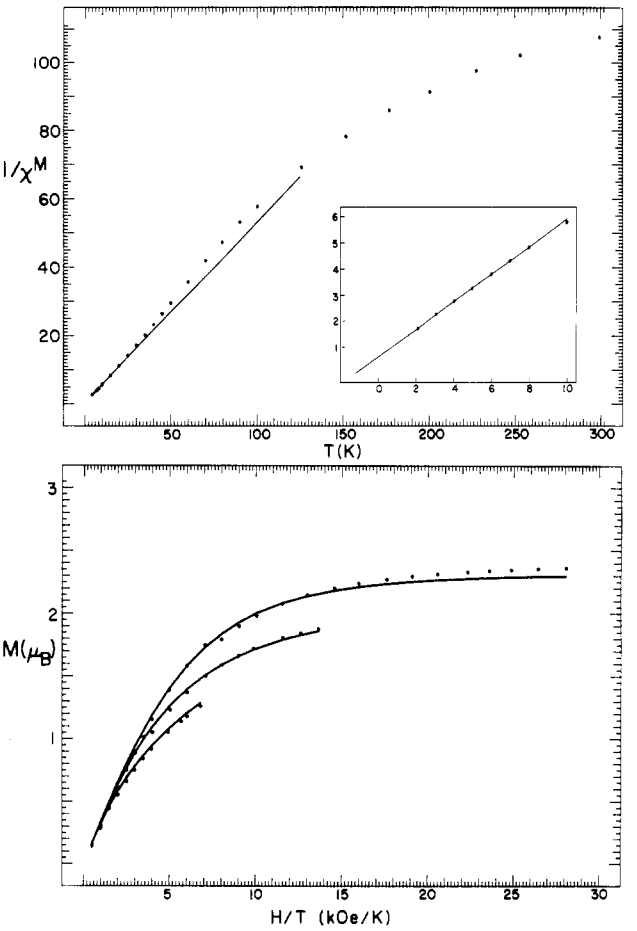

Figure 1. Upper plot: temperature dependence of the inverse molar susceptibilities (emu/mol)$^{-1}$ for $(Me_4N)_3[Fe_4S_4(SPh)_4]\cdot 2MeCN$. Solid line through the data points is a fit to the Curie–Weiss law using the parameters in Table IV. The insert is an expansion of the 2–10 K region. Lower plot: magnetization vs H_0/T at, from top to bottom, H_0 = 50, 25, and 12.5 kOe. Solid lines are theoretical fits to the data using the parameters in Table IV.

$(Me_4N)_3[Fe_4X_4(SPh)_4]\cdot 2MeCN$ (X = S, Se), which do not form isomorphous crystals yet contain clusters of very similar structures with imposed 2-fold symmetry and the same ground spin state. That state and related aspects of electronic structure have been established by methodology that is very similar to our protocol in previous studies of the electronic structures of cubane-type VFe_3S_4 and $MoFe_3S_4$ clusters[32,33] and is described in the sections that follow.

Magnetic Susceptibilities. Clusters $[Fe_4S_4(SPh)_4]^{3-}$ and $[Fe_4Se_4(SPh)_4]^{3-}$ were examined at 2–4 to 300 K. The results are plotted in Figures 1 and 2, and the selected data are listed in Table IV. At low temperatures both clusters obey the Curie–Weiss relation (1), with very small Weiss constants Θ. The

$$\chi^M = C/(T - \Theta) \qquad (1)$$

linear region of $1/\chi^M$ vs T is substantially longer for $[Fe_4Se_4(SPh)_4]^{3-}$, extending to 50 K. The Curie constants are not those for a $S = {}^1/_2$ state (C = 0.375 emu K/G) and are in good agreement with the theoretical value for $S = {}^3/_2$ (1.876 emu K/G). Above the Curie range, the two clusters behave differently, for reasons unknown. In particular, $[Fe_4S_4(SPh)_4]^{3-}$ shows a positive and then a negative deviation from eq 1, suggesting that the first-excited-state multiplet has $S = {}^1/_2$. A negative deviation from linear behavior, as shown at all temperatures above 50 K by $[Fe_4Se_4(SPh)_4]^{3-}$, is consistent with the occupancy of states

(32) Mascharak, P. K.; Papaefthymiou, G. C.; Armstrong, W. H.; Foner, S.; Frankel, R. B.; Holm, R. H. *Inorg. Chem.* **1983**, *22*, 2851.
(33) Carney, M. J.; Kovacs, J.; Zhang, Y.-P.; Papaefthymiou, G. C.; Spartalian, K.; Frankel, R. B.; Holm, R. H. *Inorg. Chem.* **1987**, *26*, 719.

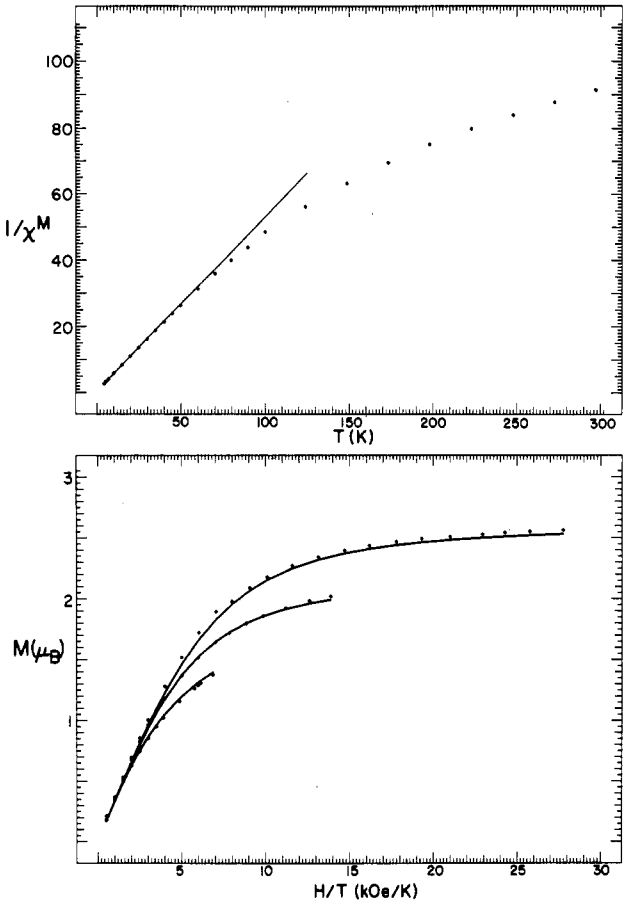

Figure 2. Upper plot: temperature dependence of the inverse molar susceptibilities $(emu/mol)^{-1}$ for $(Me_4N)_3[Fe_4Se_4(SPh)_4]\cdot 2MeCN$. Solid line through the data points is a fit to the Curie–Weiss law using the parameters in Table IV. Lower plot: magnetization vs H_0/T plotted as in Figure 1 together with theoretical fits to the data.

with $S > {}^3/_2$ or with a TIP contribution. The Se-containing cluster has the higher effective magnetic moment at room temperature. Increasing effective moment with increasing temperature also holds for salts of the oxidized clusters $[Fe_4X_4(SPh)_4]^{2-}$ (X = S, Se),[25] which have singlet ground states and thermally populated excited states arising from antiferromagnetic coupling.

Magnetization. The behaviors of the two compounds at 1.8–100 K in applied fields H_0 = 12.5, 25, and 50 kOe are shown in Figures 1 and 2. In the absence of zero-field splitting, the magnetization of an isolated spin quartet is well described by a Brillouin function with $S = {}^3/_2$ and depends only on H_0/T. However, here each cluster displays a nest of curves corresponding to different values of the applied field, indicating that the zero-field splitting parameter $D \neq 0$. Therefore, the magnetization results were treated in terms of the spin Hamiltonian (2) with $S = {}^3/_2$; E is the

$$\mathcal{H} = D[S_z^2 - S(S+1)/3] + E(S_x^2 - S_y^2) + g\mu_B\vec{H}\cdot\vec{S} \quad (2)$$

rhombic-field splitting parameter and the remaining symbols have their usual significance. The theoretical magnetization curves were generated by calculating the spin projection along the direction of the applied field. A powder average was taken by averaging this projection in equal increments of the solid angle over an octant of the unit sphere. The ratios E/D were estimated from low-temperature EPR spectra of polycrystalline solids (not shown). The only variable parameter in the calculations was D.

Best fits to the experimental data, plotted in Figures 1 and 2, are based on the spin Hamiltonian parameters in Table IV. The quality of the fits confirms the assumption of a $S = {}^3/_2$ ground state in the spin Hamiltonian of each compound. The failure of the magnetizations of the two clusters to approach more closely the limiting value $\mu = g_e\mu_B S = 3\mu_B$ at high H_0/T is due to the substantial zero-field splittings, an effect particularly noticeable for $[Fe_4S_4(SPh)_4]^{3-}$.

Table IV. Magnetic and Mössbauer Properties of $(Me_4N)_3[Fe_4X_4(SPh)_4]\cdot 2MeCN$ (X = S, Se)

property	X = S[a]	X = Se[b]
C, emu K/G	1.891	1.883
Θ, K	−1.18	−0.85
Curie–Weiss range, K	2.1–15	7.0–50
μ, μ_B (T, K)	3.13 (2.08)[c]	
	3.48 (4.18)	3.35 (4.17)
	3.78 (10.00)	3.72 (10.00)
	3.76 (25.00)	3.83 (25.00)
	3.68 (50.01)	3.89 (49.80)
	3.73 (100.2)	4.06 (99.95)
	3.94 (151.7)	4.34 (148.8)
	4.19 (200.3)	4.59 (198.2)
	4.45 (253.0)	4.86 (247.9)
	4.72 (299.4)	5.10 (297.1)
D, cm^{-1}	4.74	2.69
$\lvert E/D\rvert$	0.17	0.33
δ,[d] mm/s (4.2 K)	0.43	0.44
ΔE_Q, mm/s (4.2 K)	0.94[g]	0.92[g]
η	0.67	0.61
Γ, mm/s	0.40	0.34
A_x, mm/s	0.727[e]	0.797
A_y, mm/s	0.288	0.298
A_z, mm/s	0.618	0.402
H_x, H_y, H_z, kOe		
H_0 = 60 kOe	−131, −59, −52[f]	−144, −63, −53
H_0 = 80 kOe	−142, −61, −69	−158, −64, −66

[a,b] Diamagnetic corrections (cgsu/mol × 10^{-6}): (*a*) −710; (*b*) −749. [c] Measured at 100 G; all other data at 5 kG; moments calculated from the Curie law, μ (μ_B) = $2.828(\chi^M T)^{1/2}$. [d] Relative to Fe metal at 4.2 K. [e] Magnetic hyperfine parameters for the 14.4 keV excited state of ^{57}Fe. [f] Negative hyperfine fields oppose the applied field. [g] $V_{zz} > 0$.

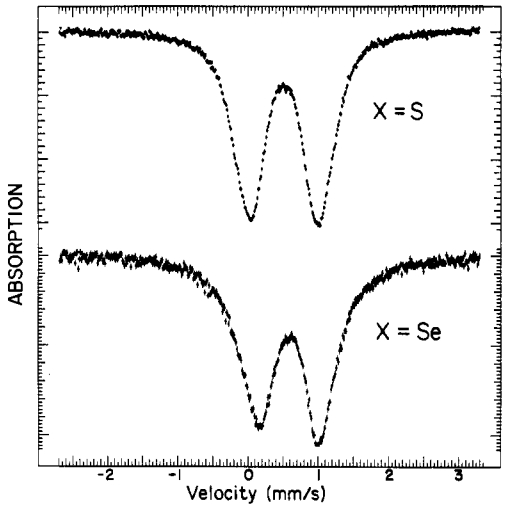

Figure 3. Mössbauer spectra of $(Me_4N)_3[Fe_4X_4(SPh)_4]\cdot 2MeCN$ (X = S, Se) in zero applied magnetic field at 4.2 K. A least-squares theoretical fit to the data yielded the parameters in Table IV.

Mössbauer Spectra. Spectra in zero applied magnetic field are shown in Figure 3. Spectral parameters for zero field and magnetically perturbed spectra affording best fits to the experimental data are collected in Table IV. At 4.2 K spectra of the two clusters consist of a single pair of relatively broad, quadrupole-split lines (Γ = 0.5–0.6 mm/s). Spectra at 80 K (not shown) have considerably narrower and more symmetric line shapes. We attribute the large line widths and the left-to-right asymmetry in the 4.2 K spectra to residual unresolved paramagnetic hyperfine structure that decreases because of faster relaxation rates at higher temperatures. Isomer shifts of the two clusters are indistinguishable despite the differences in chalcogenide atom and are in agreement but on the low side of those determined for other $[Fe_4S_4(SR)_4]^{3-}$ clusters.[5,7,10,12] Similarly, isomer shifts of native Fd and Se–Fd from *Clostridium pasteurianum* are essentially the same, and the shifts of these reduced proteins[19,22] (0.40–0.45 mm/s) and the reduced Fe protein of *Azotobacter vinelandii*

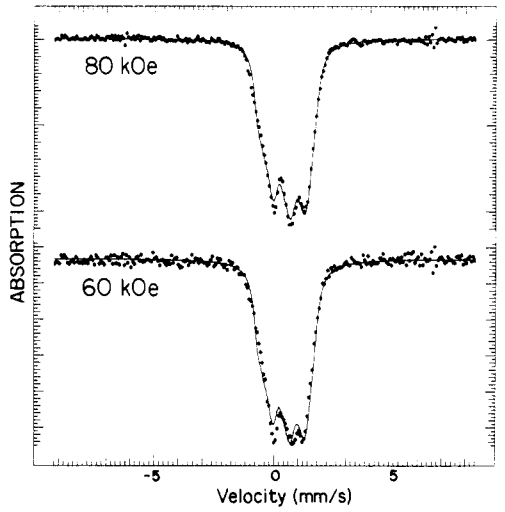

Figure 4. Magnetically perturbed Mössbauer spectra of $(Me_4N)_3[Fe_4S_4(SPh)_4]\cdot 2MeCN$ at $H_0 = 60$ and 80 kOe and 4.2 K. The solid line is a fit to the data with use of the parameters in Table IV.

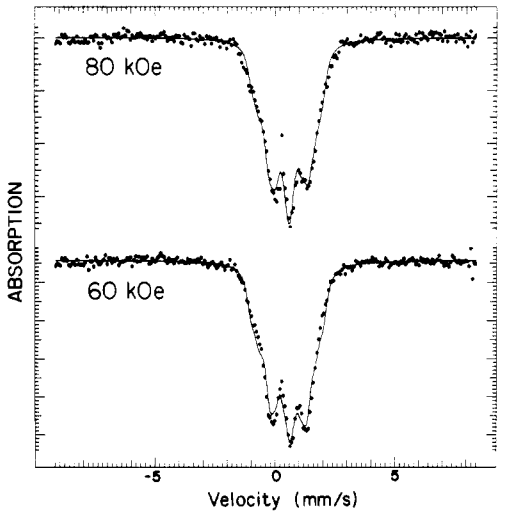

Figure 5. Magnetically perturbed Mössbauer spectra of $(Me_4N)_3[Fe_4Se_4(SPh)_4]\cdot 2MeCN$ at $H_0 = 60$ and 80 kOe and 4.2 K. The solid line is a fit to the data with use of the parameters in Table IV.

nitrogenase[23] (0.41–0.46 mm/s) conform closely to those of the analogue clusters.

Experimental and theoretical spectra of the two clusters in applied fields of 60 and 80 kOe at 4.2 K are presented in Figures 4 and 5. Under these conditions the clusters manifest collapsed spectra with an overall spread of about 3 mm/s. This indicates near cancellation of the applied field by the hyperfine fields at the ^{57}Fe nuclei. The spectra were fitted by least-squares methods using the spin Hamiltonian (2) and parameters fixed by the magnetization and EPR results. The fits were performed in the limit of fast relaxation with a single set of parameters corresponding to a model having four equivalent Fe sites in each cluster. A powder average was taken with random crystalline orientation being assumed in the sample. The quantization axis was taken to be that of the electric field gradient (EFG), assumed parallel at all four sites. The variables in the calculations were the signs of V_{zz} (the principal component of the EFG), the asymmetry parameter $\eta = (V_{xx} - V_{yy})/V_{zz}$, and the magnetic hyperfine coupling constants A_x, A_y, and A_z. Separate attempts to analyze the spectra, in terms of two sites or with a single site and magnetic hyperfine axes rotated with respect to the EFG axes, did not significantly improve the fits. We note, however, that crystal structures (vide infra) show that, at least at ambient temperature, the Fe atoms are inequivalent in pairs. Magnetic hyperfine fields at the Fe nucleus were calculated from the spin Hamiltonian parameters and magnetic hyperfine coupling constants. Results

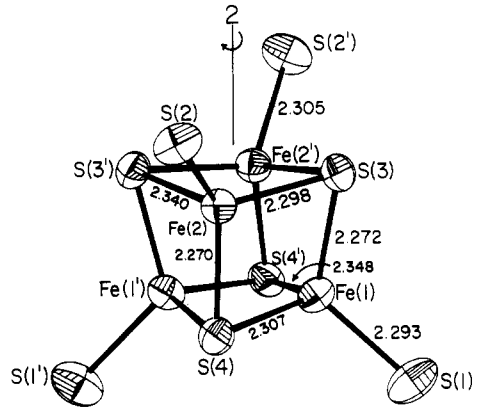

Figure 6. Structure of $[Fe_4S_4(SPh)_4]^{3-}$ showing the atom-labeling scheme, 50% probability ellipsoids, selected interatomic distances (Å), and the location of the crystallographically imposed C_2 axis, which relates primed and unprimed atoms.

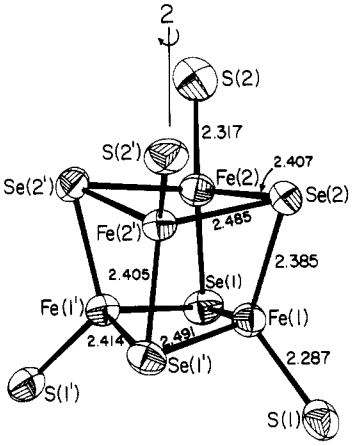

Figure 7. Structure of $[Fe_4Se_4(SPh)_4]^{3-}$, conveying the same information as in Figure 5.

are shown in Table IV. Although the coupling constants themselves show no obvious symmetry, it appears that the magnetic hyperfine interaction has near-uniaxial symmetry about an axis perpendicular to V_{zz}.

Magnetic Mössbauer spectra provide a simple means of distinguishing $S = {}^1/_2$ and ${}^3/_2$ ground states. Among analogue clusters, $[Fe_4S_4(S\text{-}p\text{-}C_6H_4Br)_4]^{3-}$ as its Et_4N^+ salt is the prototypical $S = {}^1/_2$ cluster.[10,12] Its high-field spectrum requires two sites of equal intensity but with magnetic hyperfine parameters of differing magnitudes and of *opposite* sign, as found for spin-doublet biological clusters.[23,34,35] The spectra in Figures 4 and 5, characterized mainly by reduced magnetic splittings in large applied fields, are decidedly similar to those of $S = {}^3/_2$ clusters of the nitrogenase Fe protein[23] and of Se–Fd_{red}[22] taken in comparable applied fields. This work fully sustains the correlation between the spectra of the native clusters and the quartet spin state.

Structures of $[Fe_4X_4(SPh)_4]^{3-}$. The compounds $(Me_4N)_3[Fe_4X_4(SPh)_4]\cdot 2MeCN$ crystallize in monoclinic space group $C2/c$ (X = S) and orthorhombic space group $Fdd2$ (X = Se), each with a C_2 axis imposed on the cluster anion. The cations and solvate molecules are unexceptional and are not considered further. Cluster structures are depicted in Figures 6 and 7, and selected metric data are compiled in Table V. The clusters exhibit the familiar cubane-type stereochemistry. Because compounds of this type have been previously described by us at some length,[2,5,6,10,11,24,25] only the most significant structural aspects of

(34) Middleton, P.; Dickson, D. P. E.; Johnson, C. E.; Rush, J. D. *Eur. J. Biochem.* **1978**, *88*, 135.
(35) Christner, J. A.; Münck, E.; Janick, P. A.; Siegel, L. M. *J. Biol. Chem.* **1981**, *256*, 2098.

Table V. Selected Interatomic Distances (Å) and Angles (deg) for $(Me_4N)_3[Fe_4X_4(SPh)_4]\cdot 2MeCN$, X = S (**1**), Se (**2**)

1		2	
	Core		
Fe(1)–S(3)	2.272 (2)	Fe(1)–Se(2)	2.385 (1)
Fe(2)–S(4)	2.270 (2)	Fe(2)–Se(1)	2.405 (1)
Fe(1)–S(4)	2.307 (2)	Fe(1)–Se(1)	2.414 (1)
Fe(2)–S(3)	2.298 (2)	Fe(2)–Se(2)	2.407 (1)
Fe(1)–S(4′)	2.348 (2)	Fe(1)–Se(1′)	2.491 (1)
Fe(2)–S(3′)	2.340 (1)	Fe(2)–Se(2′)	2.485 (1)
Fe(1)–Fe(1′)	2.722 (2)		2.719 (2)
Fe(1)–Fe(2)	2.720 (1)		2.782 (1)
Fe(1)–Fe(2′)	2.757 (1)		2.809 (1)
Fe(2)–Fe(2′)	2.706 (1)		2.802 (2)
S(3)···S(4)	3.607 (2)	Se(1)···Se(2)	3.808 (1)
S(3)···S(4′)	3.627 (2)	Se(1)···Se(2′)	3.910 (1)
S(3)···S(3′)	3.729 (3)	Se(1)···Se(1′)	4.031 (1)
S(4)···S(4′)	3.741 (3)	Se(2)···Se(2′)	3.965 (1)
Fe(1)–S(3)–Fe(2)	73.06 (5)	Fe(1)–Se(1)–Fe(1′)	67.32 (5)
Fe(2)–S(3)–Fe(1′)	73.42 (5)	Fe(1)–Se(1)–Fe(2)	70.51 (4)
Fe(2)–S(3)–Fe(2′)	71.40 (5)	Fe(2)–Se(1)–Fe(1′)	69.98 (4)
Fe(1)–S(4)–Fe(1′)	71.58 (5)	Fe(1)–Se(2)–Fe(2)	70.98 (4)
Fe(1)–S(4)–Fe(2)	72.93 (5)	Fe(2)–Se(2)–Fe(1′)	70.42 (4)
Fe(2)–S(4)–Fe(1′)	73.25 (5)	Fe(2)–Se(2)–Fe(2′)	69.88 (5)
S(3)–Fe(1)–S(4)	103.95 (6)	Se(1)–Fe(1)–Se(1′)	110.52 (5)
S(4)–Fe(1)–S(3′)	103.47 (6)	Se(1)–Fe(1)–Se(2)	105.02 (2)
S(4)–Fe(1)–S(4′)	106.96 (5)	Se(2)–Fe(1)–Se(1′)	106.59 (5)
S(3)–Fe(2)–S(3′)	107.06 (5)	Se(1)–Fe(2)–Se(2)	104.61 (5)
S(3)–Fe(2)–S(4)	104.30 (6)	Se(2)–Fe(2)–Se(1′)	106.15 (5)
S(4)–Fe(2)–S(3′)	103.86 (6)	Se(2)–Fe(2)–Se(2′)	108.28 (5)
Fe(2)–Fe(1)–Fe(2′)	59.22 (6)		60.16 (5)
Fe(2)–Fe(1)–Fe(1′)	60.84 (3)		61.39 (4)
Fe(1′)–Fe(1)–Fe(2′)	59.53 (3)		60.40 (4)
Fe(1)–Fe(2)–Fe(1′)	59.62 (4)		58.21 (2)
Fe(1)–Fe(2)–Fe(2′)	61.07 (3)		59.44 (4)
Fe(2′)–Fe(2)–Fe(1′)	59.73 (3)		60.39 (4)
	Terminal Ligands		
Fe(1)–S(1)	2.293 (2)		2.287 (2)
Fe(2)–S(2)	2.305 (2)		2.317 (3)
S(1)–C(11)	1.768 (5)		1.768 (8)
S(2)–C(21)	1.763 (6)		1.772 (8)
S(1)–Fe(1)–S(3)	121.65 (7)	S(1)–Fe(1)–Se(1)	117.76 (8)
S(1)–Fe(1)–S(4)	115.08 (7)	S(1)–Fe(1)–Se(1′)	94.84 (7)
S(1)–Fe(1)–S(4′)	104.38 (6)	S(1)–Fe(1)–Se(2)	120.97 (8)
S(2)–Fe(2)–S(3)	115.80 (6)	S(2)–Fe(2)–Se(1)	122.12 (8)
S(2)–Fe(2)–S(3′)	104.27 (6)	S(2)–Fe(2)–Se(2)	116.08 (9)
S(2)–Fe(2)–S(4)	120.30 (6)	S(2)–Fe(2)–Se(2′)	98.40 (8)

the present clusters are delineated. The earlier treatments of the structure of $[Fe_4S_4(SPh)_4]^{3-}$ as its $(Et_3MeN)^+$ salt[5] and of $(Et_4N)_3[Fe_4S_4(SCH_2Ph)_4]$[6] are particularly pertinent in this respect.

(a) Cores. The imposed C_2 axes pass through the centroids of opposite, nonplanar Fe_2X_2 faces of the $[Fe_4X_4]^+$ cores of the clusters. Under crystallographic C_2 symmetry there are two independent Fe and X atoms and thus six independently bonded Fe–X distances. However, the structures can be idealized with retention of essential information. The Fe–X bond lengths can be partitioned into sets of four "long" plus eight "short" whose mean values are 2.344 (6) Å + 2.287 (19) Å and 2.488 (4) Å + 2.403 (12) Å for X = S and Se, respectively. The cores assume an *elongated* tetragonal (D_{2d}) distortion from cubic symmetry in which the 2-fold axis is approximately perpendicular to the direction of elongation defined by an idealized $\bar{4}$ axis. Other bond distances and angles fall within normal ranges. Nonbonded X···X separations in similar clusters often reflect rather clearly the idealized core symmetry. However, in these cases they do not closely conform to elongated D_{2d} symmetry, under which these distances divide into two short (perpendicular to the $\bar{4}$ axis) and four long (in faces parallel to the $\bar{4}$ axis). Instead, the spread of distances of the latter type is 0.11 Å. The volumes of the $[Fe_4X_4]^+$ cores, 9.63 Å^3 (+0.8%, X = S) and 10.69 Å^3 (+1.4%, X = Se) have increased (by the indicated amounts) compared to those present in the oxidized clusters $[Fe_4X_4(SPh)_4]^{2-}$,[24,25] a behavior always found upon reduction of $[Fe_4X_4]^{2+}$ cores.

(b) Terminal Ligands. In the core series $[Fe_4S_4]^{3+,2+,+}$ it has been established that the Fe–SR bond distances lengthen as the Fe(II) character of the core increases.[2,10,11,36] The latter causes an increase in the effective radius of the Fe atom. This trend is followed by the present clusters. Relative to $[Fe_4X_4(SPh)_4]^{2-}$, mean bond lengths have increased from 2.263 (7)[24] to 2.295 (7) Å (X = S) and from 2.273 (7)[25] to 2.302 (21) Å (X = Se). The Fe sites are distorted in an angular sense from C_{3v} local symmetry. For each independent Fe atom there is one relatively small RS–Fe–X angle and two substantially larger ones. With $[Fe_4Se_4(SPh)_4]^{3-}$ the effect is more pronounced, the smaller angles being 94.84 (7) and 98.40 (8)° and the other angles being >116°. These have the effect of bending the two Fe–S bonds toward Fe–X core edges containing the same Fe atom in a manner consistent with C_2 symmetry. In both oxidized and reduced clusters, angles external to the core are notoriously variable, presumably because of packing forces acting on the (usually) large R substituent. In $(Me_4N)_2[Fe_4S_4(SPh)_4]$,[24] for example, these angles cover a range of 35°!

Spin States and Structures. The structures of $[Fe_4X_4(SPh)_4]^{2-,3-}$ clusters are schematically compared in Figure 8 with emphasis on core stereochemistry as set by Fe–X bond lengths. As is the case with most oxidized clusters, $[Fe_4X_4(SPh)_4]^{2-}$ (X = S, Se) as their Me_4N^+ salts exhibit four short and eight long Fe–X bonds, corresponding to *compressed* tetragonal distortion with the idealized $\bar{4}$ axis being the direction of compression. One-electron reduction of both clusters retains their idealized D_{2d} symmetry but changes the sense of the distortion from compressed to elongated, with the elongation parallel to the $\bar{4}$ axis. This result has been observed for $[Fe_4S_4(SPh)_4]^{3-}$ in *three* crystalline environments, two of them in the $(Et_3MeN)^+$ salt. The structure of $[Fe_4Se_4(SPh)_4]^{3-}$ is the first available for a $[Fe_4Se_4]^+$ cluster. Some time ago, on the basis of comparative solid-state and solution properties, we suggested that the conversion from a compressed to an elongated arrangement is the intrinsic structural change upon reduction of an oxidized cluster.[5]

There has not yet emerged a clear correlation between core structure and spin ground state. If such a correlation does exist, is likely to be secured only from analogue structures because of the relative accuracy of their structure determinations. It must be borne in mind, however, that structures have been determined at room temperature, while the magnetic properties that identify spin state have been established at cryogenic temperatures. While the clusters presented here clearly have $S = {}^3/_2$ states, $[Fe_4S_4(SPh)_4]^{3-}$ in its $(Et_3MeN)^+$ salt, with a nearly identical tetragonal distortion, does not have a pure quartet ground state.[5] Recent research has shown that this compound belongs to a newly recognized group in which the reduced clusters have a spin-admixed ground state. These clusters lack the Mössbauer spectral features of $S = {}^1/_2$ species and exhibit at very low temperatures and high magnetic fields saturation magnetization at values intermediate between those of $S = {}^1/_2$ and ${}^3/_2$ clusters.[37] The one compound exhibiting a pure $S = {}^1/_2$ ground state, $(Et_4N)_3[Fe_4S_4(S\text{-}p\text{-}C_6H_4Br)_4]$,[12] displays a somewhat irregular core that can be reasonably idealized to compressed tetragonal symmetry.[10]

Reduced clusters with $S > {}^1/_2$ ground states have now been identified in at least three cases: clostridial Se–Fd_{red},[15-22] the Fe protein of *A. vinelandii* nitrogenase,[23] an amidotransferase from *Bacillus subtilis*,[38] and the oxidized form of the "P-clusters" of nitrogenase[39] (assuming, as current evidence suggests, that these

(36) O'Sullivan, T.; Millar, M. M. *J. Am. Chem. Soc.* **1985**, *107*, 4096.
(37) Carney, M. J.; Papaefthymiou, G. C.; Spartalian, K.; Frankel, R. B.; Holm, R. H., to be submitted for publication.
(38) Vollmer, S. J.; Switzer, R. L.; Debrunner, P. G. *J. Biol. Chem.* **1983**, *258*, 14284.
(39) (a) Huynh, B. H.; Henzl, M. T.; Christner, J. A.; Zimmermann, R.; Orme-Johnson, W. H.; Münck, E. *Biochim. Biophys. Acta* **1980**, *623*, 124. (b) Johnson, M. K.; Thomson, A. J.; Robinson, A. E.; Smith, B. E. *Biochim. Biophys. Acta* **1981**, *671*, 61. (c) Smith, J. P.; Emptage, M. H.; Orme-Johnson, W. H. *J. Biol. Chem.* **1982**, *257*, 2310.

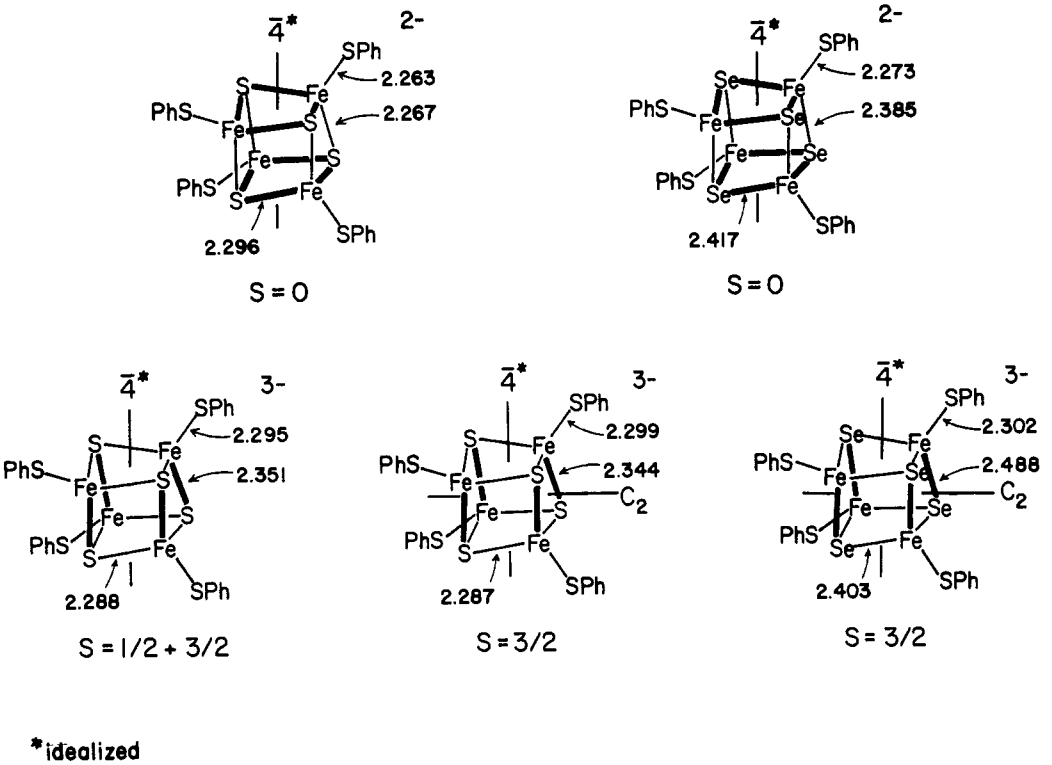

Figure 8. Schematic representations of the structures of clusters in $(Me_4N)_2[Fe_4X_4(SPh)_4]$[24,25] (top) and $(Et_3MeN)_3[Fe_4S_4(SPh)_4]$[5] and $(Me_4N)_3[Fe_4X_4(SPh)_4]\cdot 2MeCN$ (bottom); X = S, Se. Mean values of long and short Fe–X core bonds and Fe–S terminal bonds, crystallographic and idealized (*) symmetry axes, and ground spin states are indicated.

are $[4Fe\text{–}4S]^+$ clusters). The latter appear to have a $S = {}^5/_2$ ground state. A similar cluster may also be present in *C. pasteurianum* hydrogenase II.[40] The Fe protein is especially interesting because its distribution over doublet and quartet states is dependent on an extrinsic variable, the solvent medium. Thus, addition of hexamethylphosphoramide or ethylene glycol shifts the distribution toward the $S = {}^1/_2$ form, while the reverse is true in 0.4 M urea. The conclusion is inescapable that changes in structure of the two subunits to which the cluster is bound are transmitted to the cluster in such a way as to shift spin-state distribution, a matter stated in equivalent terms by Lindahl et al.[23] In analogue chemistry, corresponding circumstances may be produced by crystal lattice forces, which structurally influence the cluster toward a particular spin state. It is not yet known if spin-state differences will be manifested in core features or associated with terminal-ligand conformations. The real situation may turn out to be much more subtle than that. If our analysis of the magnetism of oxidized and reduced clusters,[41] based on the standard exchange Hamiltonian $\mathcal{H} = -2\sum J_{ij}\vec{S}_i\cdot\vec{S}_j$, is accepted, the results show that the order of spin levels is dependent on the ratio of two coupling constants J_1 and J_2. We noted that when the difference between negative J values exceeds only ca. 35%, a quartet state becomes the ground state in this model. The structural features that would produce such a difference are neither evident nor predictable at this stage of investigation of the problem.

Future reports will deal with the properties of reduced clusters with spin-admixed ground states and provide an expanded consideration of the relation between the structures and spin ground states of reduced clusters.[37] In this report, we have provided unequivocal evidence using compounds whose compositions and structures are beyond question that *the reduced clusters* $[Fe_4X_4(SPh)_4]^{3-}$ *(X = S, Se) can stabilize electronic configurations with spin-quartet ground states.* As with the findings of our prior study of $[Fe_4S_4(SC_6H_{11})_4]^{3-}$,[12] results of this investigation fully substantiate the conclusion that the reduced Fe protein of nitrogenase contains a spin-quartet cluster. As yet, clusters with ground state spins $S > {}^3/_2$ have been claimed only in Se–Fd_{red} and the P clusters of nitrogenase.

Acknowledgment. This research was supported at Harvard University by NIH Grant 28856 and at MIT by the National Science Foundation.

Registry No. $(Me_4N)_3[Fe_4S_4(SPh)_4]\cdot 2MeCN$, 111933-57-4; $(Me_4N)_3[Fe_4Se_4(SPh)_4]\cdot 2MeCN$, 111958-53-3; $(Me_4N)_2[Fe_4S_4(SPh)_4]$, 53260-80-3; $(Me_4N)_2[Fe_4Se_4(SPh)_4]$, 66416-78-2.

Supplementary Material Available: Tabulated temperature dependencies of susceptibilities, positional and thermal parameters, hydrogen atom positional parameters, and interatomic distances and angles (8 pages); tabulated calculated and observed structure factors (41 pages). Ordering information is given on any current masthead page.

(40) Rusnak, F. M.; Adams, M. W. W.; Mortenson, L. E.; Münck, E. *J. Biol. Chem.* **1987**, *262*, 38.
(41) Papaefthymiou, G. C.; Laskowski, E. J.; Frota-Pessôa, S.; Frankel, R. B.; Holm, R. H. *Inorg. Chem.* **1982**, *21*, 1723.